Electrical Properties of Lithium and Sodium Borate Glasses Doped with Chromium Oxide

M. A. Zaki Ewiss

Department of Physics, Faculty of Science, Cairo University, 12613 Gamaa Street, Giza, Egypt

Abstract
Background: In this work, we experimentally studied the ac-electric conductivity and dielectric constant of some lithium and sodium borate glasses doped with chromium oxide. These glass materials are of interest for science and technology.
Materials and Methods: We introduced Chromium oxide with Low concentration of 0.1 and 0.7 mol. % to Lithium and Sodium borate glasses with chemical composition 37 mol % $[M_2O]$ - 63 mol % $[B_2O_3]$ where (M=Li and Na)]).We successfully prepared the glass samples by melting quenching method. The X-ray diffraction pattern was carried out using Bruker AXS X-Ray analytical diffraction system. The ac - electrical conductivity, and dielectric constant measured at atmospheric pressure as a function of temperature (in the range from room temperature up to 500 ^0K) and frequency in the range from 0.1 kHz up to 200 kHz).
Results: The X-ray patterns showed the amorphous nature of these glasses. The curve features of the ac-conductivity showed deviations from the Arrhenius linear relation observed at T < 400 K. We estimated the crystalline activation energies for all samples under consideration. The measurements verified the scaling law of the ac-conductivity as a function of the applied frequency.
Conclusion: From the results, we have the following: a) From the recorded XRD Spectra we observed evidence of the formation of pre-crystalline phase; b) The electrical properties of these glasses are affected by the different physical and chemical processes; c) Values of the ac-conduction mechanism are predominantly ionic in the undoped samples containing Li or Na ions. The mobility of these ions is affected by the presence of Cr ions in all doped samples; d) The increase of the ionic mobility is responsible for the behaviour of the dielectric loss of these glass samples.
Keywords: alkali glasses, ac-conductivity, activation energy, dielectric constant

----
--- ---------

I.   Introduction

There is a substantial body of literature on a wealth of information aimed to study the electrical and optical properties of semiconductor glasses. These glasses are considered the most exciting materials for science and technology. They made with excellent homogeneity and in a variety of forms and size. Also, they dope with transition metal and rear earth ions. They existed with a wide range of properties which met the needs of various applications for our daily life [1-30].

During the last decades, intensive experimental and theoretical studies of Alkali borate glasses containing different transition metal oxides (TMO) were reported[1]. This wealth of information supported the development of the glass industry including the high-technology devices such as glass lasers, luminescent solar energy concentrator, optical fibres for communication devices and as a radiation shielding material etc. [1,2]. Recently, several studies reported on the physical properties of lithium borate glasses [3].

The thermochemical of lithium borate glasses are studied by high-temperature oxide melt solution calorimetry [3]. In this report, the formation enthalpies of these glasses and crystalline lithium borates were determined with typical solution behaviour. A strong exothermic acid-base reaction between Li_2O and B_2O_3 was found due to the formation of tetrahedrally coordinated boron. Sørensen et al. 4 discussed the boron anomaly in the thermal conductivity of lithium borate glasses.

Montouillout et al. [5] and Usharani & Eraiah 6 studied the ionic conductivity of lithium borate glasses and local structure probed by high-resolution solid-state NMR as well as the thermal property of holmium doped lithium lead borate glasses. For industrial application, Pawar et al. [7] and Thakur et al. [8] measured the Physical, thermal, structural and optical properties of Dy^{3+} doped lithium alumino-borate glasses for bright W-LED as well as the temperature-dependent electrical transport characteristics of $BaTiO_3$ modified lithium borate glasses. Shaaban et al. [9] studied the physical and structural properties of lithium borate glasses containing MoO_3. Moreover, Abousehly et al. [10] determined the electrical and mechanical properties of $Li_2O–BaO–B_2O_3$ glass system as a function of temperature and frequency. The results showed that the changes in Li_2O

concentration considerably affect the values of dielectric constant and dc and ac-electrical conductivities. Intensive data on the structural XRD, Raman spectroscopy, thermal (TG-DTA), dielectric, absorption and emission (Vis & NIR) properties of lithium borate glasses with and without (1 mol % Ho^{3+}) are available [11].

On the other hand, Anjaiah et al. [12] studied the dosimetric and kinetic parameters of lithium cadmium borate glasses doped with rare-earth ions. Data on the structural, thermal, dielectric and ac conductivity properties of lithium fluoro-borate optical glasses were presented and discussed [13]. These glasses were chemical composed of $Li_2O–LiF–B_2O_3–MO$ (M = Zn and Cd) and prepared by a conventional melt quenching method. Gedam and Ramteke [14] presented information on the Electrical and optical properties of lithium borate glasses doped with Nd_2O_3. Also, Funke and Banhatti [15] investigated the frequency-dependent conductivities and permittivities. In previous reports, the electrical, IR- spectroscopy, and DTA of some sodium tetraborate glasses containing vanadium and ferric oxides as well as the dielectric spectroscopy of [98 mol%$(Na_2B_4O_7)$ – 2mol%(Cr_2O_3)] and [98mol%$(Na_2B_4O_7)$ – 2mol%(MnO)] semiconductor glasses were measured and discussed [16-18].

The objective of the present work is to study the effect of adding a low concentration of chromium oxide on the electrical behaviour of some Lithium and Sodium borate glasses. The magnitude of ac-electrical conductivity, dielectric loss, and verification of the empirical laws of the ac-conductivity as a function of temperature and frequency as well as the activation energies of all glass samples under consideration will be presented and discussed.

II. Experimental arrangement

II-1) Glass preparation

In this experiment, we used analytical grade chemicals for the preparation of the glasses samples. In **Table 1**, the chemical composition of the glasses under consideration, including the density ρ (g/cm^3), specific volume (V_s) and molar volume (V_m) is given. The batch of all components is calculated and weighted.

Table 1, Composition of glass samples

Sample No.	Glass Composition (mol %)				Density ρ (g/cm³)	Specific volume (V_s)	Molar volume (V_m)
	B_2O_3	Li_2O	Na_2O	Cr_2O_3			
1	63	37	--	--	2.08	0.48	47.15
2	62.9	37	--	0.1	2.27	0.44	109.75
3	62.5	37	--	0.7	2.36	0.42	104.76
4	63	--	37	--	2.21	0.45	59.21
5	62.9	--	37	0.1	2.36	0.42	118.76
6	62.3	--	37	0.7	2.75	0.36	101.8

We added the Boron oxide in the form of orthoboric acid H_3BO_3, the metal oxide as a hydrous carbonate M_2CO_3 where (M=Li, and Na) and Cr_2O_3 oxide as it is. The weight batches were melted in an electrically heated furnace at $1100 \pm 10\ ^0C$ for 2 hours and with stirring of the melt at intervals to achieve acceptable homogeneity. Attention was paid to reducing the mechanical and volatilization losses. The homogenous melt was finally poured in a clean stainless steel plate and cast into disks of about 2 cm diameters and 2 mm thickness. The disks were immediately transferred to another furnace adjusted at 400 ^0C for one hour for annealing and then switch off the temperature to cool down gradually to room temperature with a cooling rate of 0.5 ^{0}C/min. The glass samples were polished using the polishing paper [1].

II-2) Electrical measurements

Both the dielectric constant and ac - electrical conductivity are measured as follows:
1. The silver paste was carefully used to make two circular electrodes on both sides of the glass sample under consideration (see Table 1).
2. The sample was placed between two copper plates mounted inside the heat stage with four probes (to eliminate any stray capacitance).
3. The ac - electrical conductivity (σ_{ac}) and dielectric constant (ε) were measured at atmospheric pressure as a function of temperature (in the range from room temperature up to 500 ^{0}K) and frequency in the range from 0.1 kHz up to 200 kHz).

4. The heating rate of 0.5 ^{O}C/min was controlled using platinum resistance (PT1000). The sample temperature was measured using the other two platinum resistance (PT1000) resistance placed at the surface of the electrodes.
5. The LCR –Hioki bridge determines the accuracy of the measurement.
6. The value of the ac-electric conductivity of the sample under consideration was extracted as follows:
7. The capacitance C in Farad and the conductance G in Siemens are measured using the Hioki –Bridge (model Hioki 3535 LCR HiTester) at different frequencies (f in Hz).

The complex dielectric constant ε* = ε'- iε" are calculated at angular frequency ω = 2πf, where ε' and ε" are the real and imaginary part of the dielectric constant from equation 1 and 2 given by the following equations [1]:

$$\epsilon' = {dc}/{\epsilon_o A} \tag{1}$$

and

$$\epsilon" = {dG}/{\epsilon_o A\omega} \tag{2}$$

Here d is the thickness of the sample, and A is the area of the electrode.
The real σ_{ac}' and the imaginary $\sigma_{ac}"$ parts of the ac- electrical conductivity is calculated from the following equations [1]:

$$\sigma_{ac}' = \omega\epsilon_o\epsilon" \tag{3}$$

and

$$\sigma_{ac}" = \omega\epsilon_o\epsilon' \tag{4}$$

It is worth mentioning that in this experiment, all the measurements were reproducible.

III. Results And Discussion

III-1) X-Ray Diffraction Spectra

The X-ray diffraction (XRD) pattern was carried out using Bruker AXS X-Ray analytical diffraction system; type D8 advanced Theta/2 Theta standard supplied with furnace attachment on the powder samples at room temperature (T=298 K) and T=393^{0}K. The target was Cu K$_{\alpha}$ radiation with K$_{\alpha 1}$=1.54060 A^{0}, K$_{\alpha 2}$=1.54439 A^{0} and K$_{\alpha 3}$=1.1.39222 A^{0}. The angular (2θ) started at 4^{0} and ended at 70^{0} with applied voltage was of K.V. and anode current of 40 mA. The detailed measurements were performed by a stepwise measuring method with a step rate 0.02^{0} and stepped time 0.4 s. the data were analyzed by looking up a match of all major peaks with the JCPDS cards (JCPDS = joint committee on powder diffraction stander).

The X-ray diffraction pattern for glass sample 1 of [37mol% Li$_2$O+63mol% B$_2$O$_3$] and glass sample 2 of [37mol% Na$_2$O+63mol% B$_2$O$_3$] at room temperature T= 298^{0}K, showed the absence of the crystalline nature, see Figure 1a and Figure 1c, respectively.
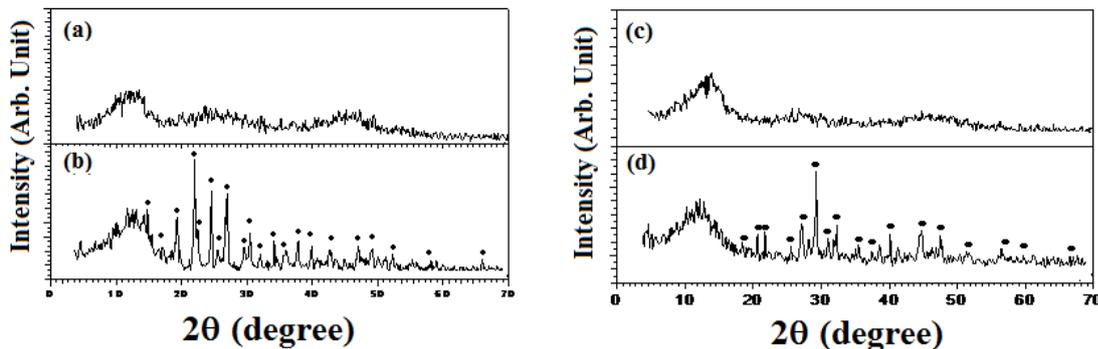

Figure 1: X-ray diffraction pattern for

a) **[37 mol % Li$_2$O +63 mol % B$_2$O$_3$] glass at T = 298 K**
   b)
c) **[37 mol % Li$_2$O +63 mol % B$_2$O$_3$] glass at T = 393 K**
d) **[37 mol% Na$_2$O +63 mol % B$_2$O$_3$] glass at T = 298 K**
e) **[37 mol% Na$_2$O +63 mol % B$_2$O$_3$] glass at T = 393 K**

From Figure 1b, at T=393 K the d-spacing that are associated with the heat-treated of the [37 mol % Li_2O+63 mol % B_2O_3] (sample 1) are located at 5.819, 4.76, 4.56, 4.48, 3.961, 3.557, 3.42, 3.362, 3.292, 3.252, 2.97, 2.89, 2.76, 2.59, 2.42, 2.35, 2.23, 2.19, 2.157, 1.919, 1.840, 1.730, 1.550 and 1.430, these peaks are matches with lithium borate peaks of the two phases ($Li_2B_8O_{13}$ and $Li_2B_{10}O_{16}$. H_2O). From Figure 1d, at T=393 K for [37 mol % Na_2O+63 mol % B_2O_3] sample4, the d- spacing are located at 7.72, 6.68, 4.88, 4.48, 3.71, 3.55, 3.47, 3.26 and 3.13 corresponds to α-$Na_2B_6O_{10}$ monoclinic system The d-spacing located at 3.47, 3.27, 2.825, 2.77, 2.57, 2.12, 2.02, and 1.92 corresponds to $Na_2B_4O_7$ orthorhombic system, while the d-spacing located at 3.97, 3.03, 2.85, 2.64, 2.51, and 2.31 are attributed to sodium borate hydrate $NaBO_3.4H_2O$ triclinic system. Although the formation of these crystalline systems was found, there is an incomplete periodic structure which indicates the existence of a pre crystalline phase. We need more experimental and theoretical investigation, including Raman spectroscopy, NMR and laser-induced fluorescence techniques, to clarify the existence of this pre-crystalline phase.

III-2) Measurements of ac-electrical conductivity

III-2-1) Undoped Alkali Borate Glasses

In Table 2, the values of the measured real (σ_{ac}') and imaginary (σ_{ac}'') parts of the ac electrical conductivity at different frequencies and room temperature of 298^0 K for all samples under consideration are given, respectively. For the [37 mol % Li_2O+63 mol % B_2O_3] undoped glass sample1, the values of σ_{ac}' and σ_{ac}'' at room temperature (T = 298^0 K) and at low frequency of 100 Hz are equal to 3.39×10^{-8} mho.m^{-1} and 8.49×10^{-8} mho.m^{-1} respectively. These values are increased by increasing the applied frequency. At a frequency of 200 kHz, they increased by two and four orders of magnitude, respectively.

Table 2: The values of the real and imaginary parts of ac electrical conductivity and dielectric constant at room temperature (T = 298 K) at different frequencies for all samples (see Table 1).

Sample No.	F (KHz)	σ_{ac}' (298 K) $\Omega^{-1}m^{-1}$	σ_{ac}'' (298 K) $\Omega^{-1}m^{-1}$	ε'	ε''
(1)	0.1	3.39×10^{-8}	8.49×10^{-8}	15.23	6.07
	1	6.72×10^{-7}	6.73×10^{-7}	12.08	1.30
	10	1.48×10^{-7}	6.46×10^{-6}	11.58	0.27
	21	2.15×10^{-7}	1.38×10^{-5}	11.50	0.18
	100	5.39×10^{-7}	6.36×10^{-5}	11.41	0.18
	216	1.01×10^{-6}	1.37×10^{-4}	11.37	0.08
(2)	0.1	4.40×10^{-10}	4.94×10^{-8}	8.89	0.08
	1	2.13×10^{-9}	4.91×10^{-7}	8.82	0.04
	10	1.25×10^{-8}	4.88×10^{-6}	8.78	0.02
	21	2.44×10^{-8}	1.05×10^{-5}	8.77	0.02
	100	1.14×10^{-7}	4.87×10^{-5}	8.75	0.02
	216	3.27×10^{-7}	1.05×10^{-4}	8.74	0.27
(3)	0.1	9.49×10^{-10}	5.66×10^{-8}	10.19	0.17
	1	4.90×10^{-9}	5.58×10^{-7}	10.03	0.09
	10	3.04×10^{-8}	5.53×10^{-6}	9.93	0.05
	21	5.99×10^{-8}	1.19×10^{-5}	9.90	0.05
	100	2.78×10^{-7}	5.48×10^{-5}	9.86	0.05
	216	5.97×10^{-7}	1.18×10^{-4}	9.84	0.049
(4)	0.1	2.32×10^{-9}	5.90×10^{-8}	10.62	0.42
	1	9.99×10^{-9}	5.73×10^{-7}	10.30	0.18
	10	1.18×10^{-7}	5.63×10^{-6}	10.12	0.21
	21	3.41×10^{-7}	1.20×10^{-5}	9.98	0.28
	100	1.20×10^{-6}	5.37×10^{-5}	9.65	0.21
	216	1.68×10^{-6}	1.15×10^{-4}	9.58	0.14
(5)	0.1	6.13×10^{-10}	3.96×10^{-8}	7.12	0.11
	1	2.56×10^{-9}	3.92×10^{-7}	7.02	0.04
	10	1.15×10^{-8}	3.89×10^{-6}	6.98	0.02
	21	2.25×10^{-8}	8.37×10^{-6}	6.97	0.18
	100	1.37×10^{-7}	2.25×10^{-6}	6.96	0.16
	216	2.5210^{-7}	8.34×10^{-5}	6.95	0.02
(6)	0.1	2.18×10^{-9}	5.47×10^{-8}	9.81	0.39
	1	6.80×10^{-9}	5.33×10^{-7}	9.57	0.12
	10	2.76×10^{-8}	5.27×10^{-6}	9.47	0.04
	21	5.09×10^{-8}	1.19×10^{-5}	9.45	0.04
	100	1.79×10^{-7}	5.25×10^{-5}	9.42	0.03
	216	3.63×10^{-7}	1.10×10^{-4}	9.42	0.03

From Table 2, the values of σ_{ac}' and σ''_{ac} of [37 mol% Na_2O +63 mol % B_2O_3] glass sample4 at a low frequency of 100 Hz, was found to be lower by one order of magnitude than the corresponding values of the undoped lithium borate glass (sample1). We may attribute the higher value of the conductivity of lithium borate glasses to the small size and the excellent mobility of Li - ions compared to the Na ions within the glass matrix. Also, the difference between these two conductivity values decreases by increasing the applied frequency.

The variation of $ln(\sigma'_{ac})$ as a function of reciprocal temperature are plotted at a different frequency in Figure 2(a, b) for glass sample1 and glass sample4, respectively. Figure 3(a, b) showed, the corresponding variation of $ln(\sigma''_{ac})$ as a function of the reciprocal temperature of these two samples, respectively.
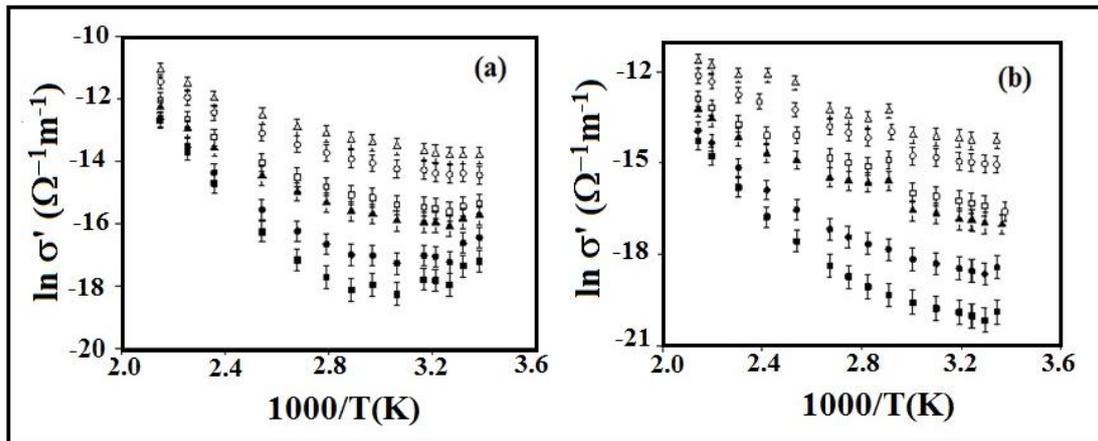
Figure 2: The relation between $ln(\sigma_{ac'})$ versus 1000/T(K) for
a) [37mol % Li_2O + 63mol % B_2O_3] glass sample1
b) [37 mol% Na_2O +63 mol % B_2O_3] glass sample4
■ 0.1 kHz ●1 kHz ▲ 10 kHz □ 21 kHz ○ 100 kHz △.200 kHz
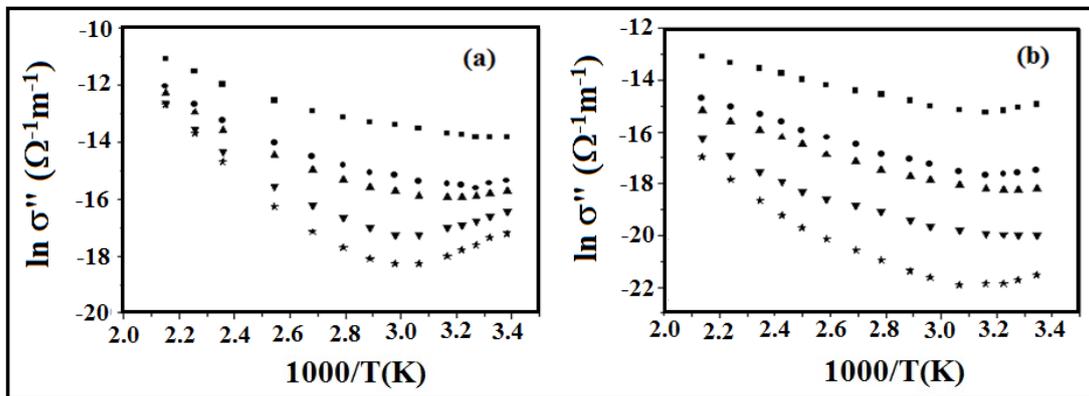
Figure 3: The relation between $ln(\sigma_{ac''})$ versus 1000/T(K) for
a) [37mol % Li_2O + 63mol % B_2O_3] glass sample1
b) [37 mol% Na_2O +63 mol % B_2O_3] glass sample4
★ 0.1 KHz ▼ 1 KHz ▲10 KHz ● 21 KHz ■.216 KHz

The ac-electrical conductivity has a non-Arrhenius behaviour over the whole temperature range between 298 and 500 K. It is worth noting that similar behaviour of ac-electrical conductivity was found for all samples under consideration. According to the Arrhenius equation given by equation [1]:

$$\sigma_{ac} = \sigma_o e^{-E_{cryst}/KT} \qquad\qquad (5)$$

Where σ_0 is constant, E_{cryst} is the activation energy, K is the Boltzman constant and T is the absolute temperature. This empirical relation represents a straight line between $ln(\sigma'_{ac})$ vs 1/T (K). We noticed that in all glass samples under consideration, this linear relation is verified in the crystalline phase at T > 400 K.

The value of E_{cryst} for all glass samples under consideration are extracted at different frequencies and is collected in Table 3, respectively.

Table 3: Values of the extracted activation energy ($E_{cryst.}$) in eV at T > 400 K

Sample No.	Glass Composition	E_{cryst}(eV)					
		Frequency (KHz)					
		0.1	1	10	21	100	216
1	37 mol % Li_2O +63 mol % B_2O_3	0.83	0.70	0.54	0.49	0.41	0.37
2	37 mol% Li_2O+62.9mol % B_2O_3+0.1 mol% Cr_2O_3	0.81	0.65	0.51	0.46	0.38	0.38
3	37 mol% Li_2O+62.3mol % B_2O_3+0.7 mol% Cr_2O_3	0.71	0.55	0.33	0.26	0.23	0.17
4	37 mol % Na_2O +63 mol % B_2O_3	0.82	0.65	0.50	0.44	0.34	0.24
5	37 mol% Na_2O+62.9mol % B_2O_3+0.1 mol% Cr_2O_3	0.73	0.67	0.41	0.28	0.29	0.26
6	37 mol% Na_2O+62.3mol % B_2O_3+0.7 mol% Cr_2O_3	0.70	0.55	0.39	0.27	0.25	0.22

We found that the value of E_{cryst} strongly depends on the applied frequency. For instance, at a frequency of 100 Hz, the value of E_{cryst} for [37mol % Li_2O + 63mol % B_2O_3] glass sample1 is 0.83 eV. This value is decreased by increasing the applied frequency. It reached a value of 0.34 at 216 kHz. Similar results are obtained for the other samples. The results for E_{cryst} with the good agreement are compared with the corresponding available data reported earlier [1,11,18,19].

We examined the deviation from the linear behaviour of the ac-electrical conductivity as a function of temperature for all samples under consideration. In this context, we used two different approaches, the small polaron hopping model (SPH) of Austin-Mott [20] and the variable range hopping model (VRH) invented by Greaves et al. [21]. According to these models neither the relation $\ln(T\sigma_{ac}')$ VS (1000/T(K)) nor $\ln(T^{1/2} \sigma_{ac}')$ VS $(1/(T(K)^{1/4})$] for both [37mol % Li_2O + 63mol % B_2O_3] and [37 mol% Na_2O +63 mol % B_2O_3] glass samples explained the deviation from the linear relation at T < 400 K. Habaski et al.[1] discussed a similar conclusion. In this context, the non-Arrhenius behaviour was attributed to the ion-ion interaction at relatively high temperatures [22,23]. On the other hand, the ion trapping model based upon the structural and chemical approach was introduced to explain the non-Arrhenius deviation in the conductivity above room temperature for fast ion conducting glasses [24]. The basic idea of this model is that the cations contributing to the ionic conduction are assumed to hop from an openly available site to the next open, accessible place within the glass matrix. The open site without any cation is considered as a negatively charged trap. In this process, mobile ions naturally by-pass unavailable filled sites and fall into traps under the circumstance that trap is open and that the ion becomes close enough to be captured by the trap. In this model, the migration distance between available traps is firmly temperature-dependent, and the ions are thermally activated according to the Boltzmann statistics. However, this model was able to reproduce the non-Arrhenius temperature dependence of the conductivity of these fast ion conducting glasses. Still the curve feature of the ac-electrical conductivity obtained for the alkali borate glass samples under consideration unexplained.

At this point, we believe that the new pre-crystalline phase observed in the recorded XRD pattern for these samples (see Figure 1) may exist during the heating process from the amorphous to the crystalline phase. We may attribute the existence of the pre-crystalline phase to the formation of the glass complexes during the thermal processing at T equal to 393 K
.

III-2-2) Alkali Borate Glasses Containing Cr_2O_3

In this experiment, low concentration of chromium oxide of concentration 0.1 mol% and 0.7 mol% was introduced to the Lithium and sodium borate glass samples under consideration (see Table 1). The values of the ac- electrical conductivity were measured as a function of temperature and applied frequency. In Figure 4 (a,b,c,d) the variation of $\ln(\sigma_{ac}')$ versus 1/T(K) for [37 mol % Li_2O+62.9 mol % B_2O_3+0.1 mol % Cr_2O_3] glass sample 2, [37 mol % Li_2O+62.5 mol % B_2O_3 + 0.7 mol % Cr_2O_3] glass sample 3, [37 mol % Na_2O+62.9 mol % B_2O_3+0.1 mol % Cr_2O_3] glass sample 5 and 37 mol % Na_2O+ 62.9 mol % B_2O_3+0.7 mol % Cr_2O_3] glass sample 6 are illustrated, respectively.

Again these curve features reflect similar non-Arrhenius behaviour as explained above. The measured values of σ_{ac}' and σ_{ac}'' of these doped glass samples at different frequencies and room temperature of 298 ^{0}K are collected in Table 2. We noticed that adding a low concentration of Cr_2O_3 to both lithium and sodium borate glasses leads to a decrease in the value of the electrical conductivity by at least one order of magnitude in the low-frequency range. This value slightly decreases at high frequency.

In figure 5(a-f), the variation of $\ln(\sigma_{ac}'')$ versus 1/T(K) is illustrated for the doped glass samples 2 and sample 3 at different frequencies, respectively. In figure 6(a-f), this variation is shown for the doped glass samples number 5 and 6.
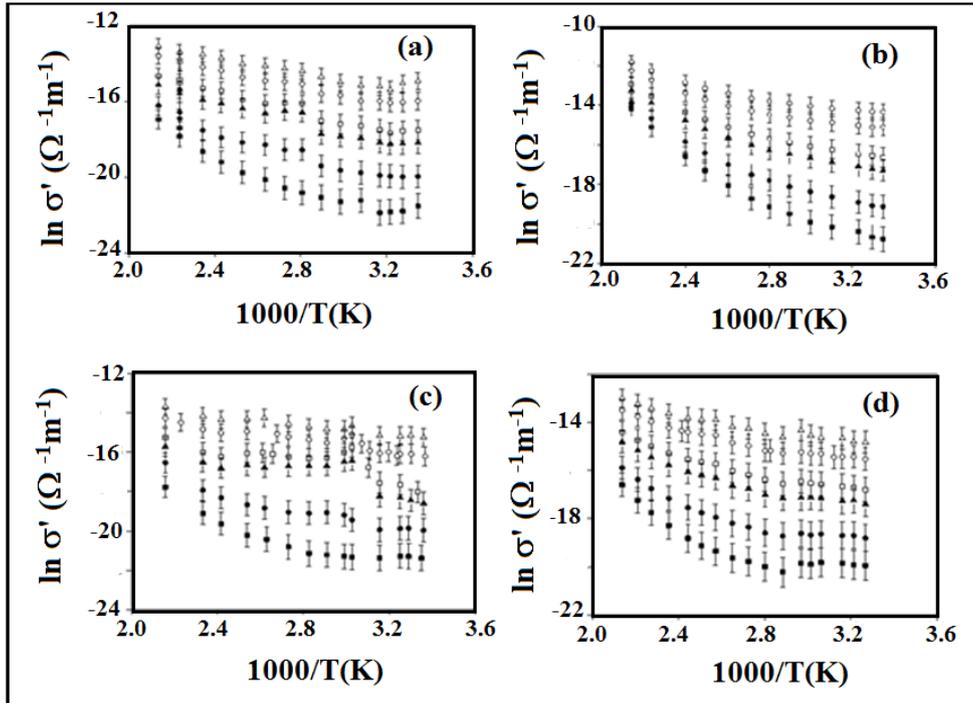
Figure 4: The relation between ln(σ$_{ac'}$) versus 1000/T(K) for
a) [37 mol % Li$_2$O+62.9 mol % B$_2$O$_3$+0.1 mol % Cr$_2$O$_3$] sample 2
b) [37 mol % Li2O+62.5 mol % B2O3 + 0.7 mol % Cr2O3] sample 3
c) [37 mol % Na$_2$O+62.9 mol % B$_2$O$_3$+0.1 mol % Cr$_2$O$_3$] sample 5
d) [37 mol % Na$_2$O+ 62.9 mol % B$_2$O$_3$+0.7 mol % Cr$_2$O$_3$] sample 6
■ 0.1 KHz   ●1 KHz ▲10 KHz □ 21KHz ○100 KHz △.200 KHz
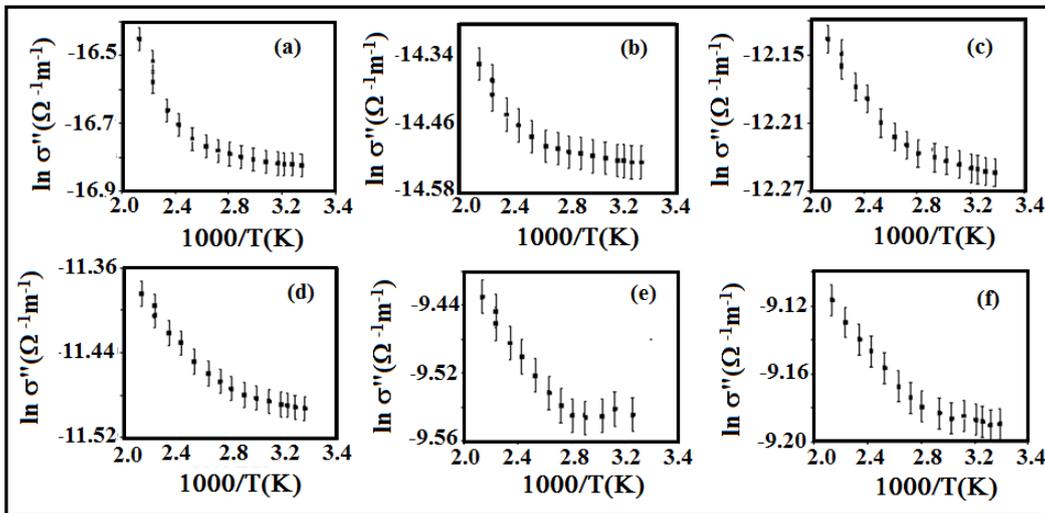
Figure 5: The relation between ln(σ$_{ac''}$) versus 1000/T(K) for
[37mol % Li$_2$O + 62.9mol% B$_2$O$_3$.+0.1mol % Cr$_2$O$_3$] glass sample.
a) 0.1 kHz   b) 1 kHz c) 10 kHz d) 21 kHz   e) 100 kHz f) 200 kHz
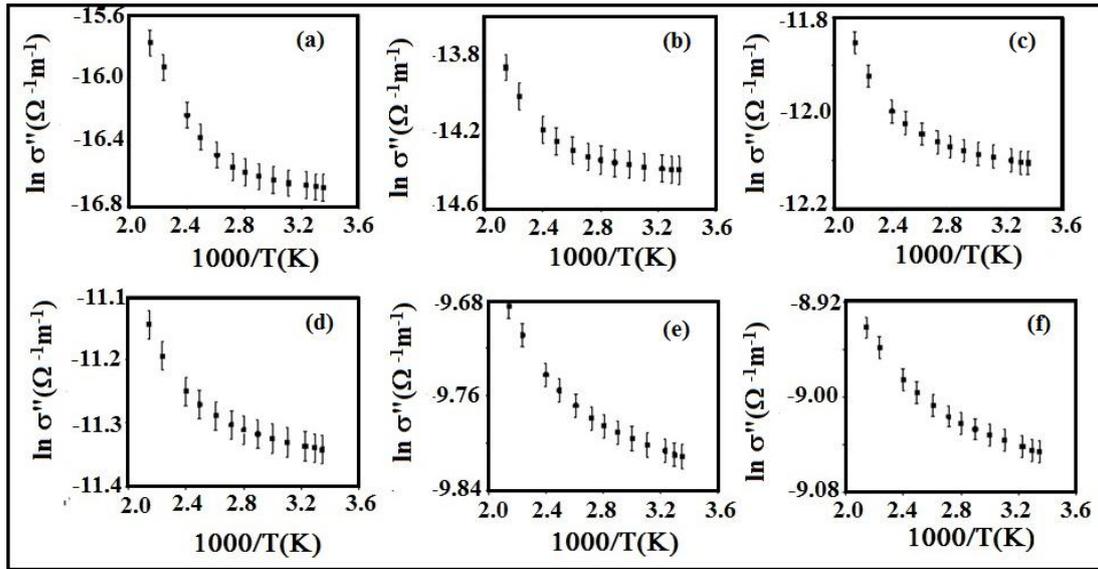
Figure 6: The relation between ln($\sigma_{ac''}$) versus 1000/T(K) for 37mol % Li$_2$O + 62.3mol% B$_2$O$_3$.+0.7 mol % Cr$_2$O$_3$] glass sample.
a) 0.1 kHz   b) 1 kHz   c) 10 kHz   d) 21 kHz   e) 100 kHz   f) 200 kHz

For comparison, the relation between ln(σ'_{ac}) vs 1000/T(K) at 1 kHz of the lithium and sodium borate glasses doped with a low concentration of chromium oxide are shown in Figure 7(a,b), respectively.
In these curves we may refer the decrease of the electrical conductivity of the doped lithium and sodium borate glass samples with a low concentration of chromium oxide to the ion-ion interactions between Cr and Li (or Na) ions and due to the formation of different complexes such as LiCrO$_3$ and NaCrO$_3$ respectively within the glass matrix. As a result of the formation of these complexes, the concentration of Li$_2$O (or Na$_2$O) is lowered within the glass matrix. Consequently, the value of σ_{ac}' and σ_{ac}'' decrease by adding Cr$_2$O$_3$— Seth et al. [26] reported similar results; they measured the electron spin resonance, optical spectra, and dc- electrical conductivity of 2Li$_2$O.3B$_2$O$_3$ glasses doped with V$_2$O$_5$ and CuO.
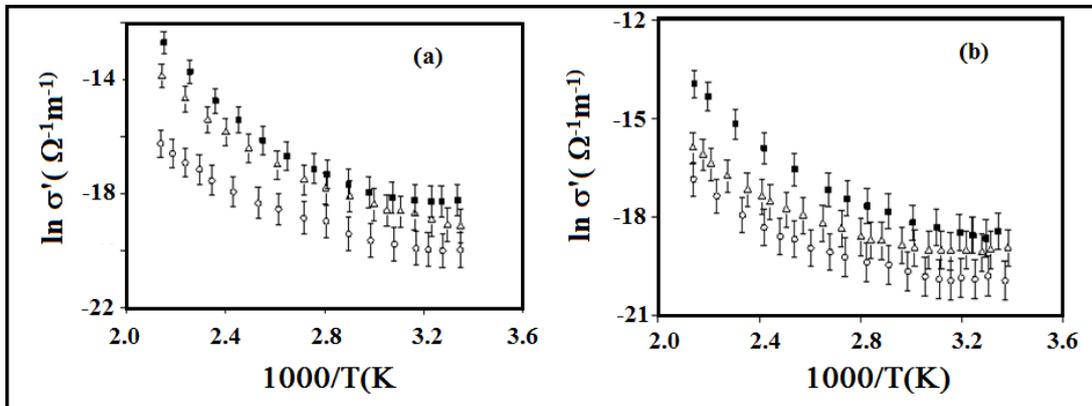
Figure 7: a) The relation between ln($\sigma_{ac'}$) versus 1000/T(K) at 1 KHz for
■[37mol % Li$_2$O +63mol % B$_2$O$_3$] sample1
○ [37mol % Li$_2$O + 62.9mol% B$_2$O$_3$+0.1mol % Cr$_2$O$_3$] sample2
Δ [37mol % Li$_2$O + 62.3mol% B$_2$O$_3$+0.7mol % Cr$_2$O$_3$] sample3
b) The relation between ln($\sigma_{ac'}$) versus 1000/T(K) at 1 KHz for
■ [37 mol% Na2O + 63mol % B2O3] sample4
○ [37 mol % Na2O + 62.9 mol % B2O3+0.1 Cr2O3] simple5
Δ [37 mol % Na2O +62.3 mol % B2O3+0.7 Cr2O3] sample6

It is worthy of mentioning that the existence of different physical and chemical processing might affect the rate of changing the conductivity by increasing the temperature. In this case, at low temperature, the ion-ion interaction and the formation of different complexes may play an essential role in decreasing the value of the

electrical conductivity. At high temperature near the crystalline stage, the hopping of the electron plays the main contribution to the conductivity.

In our case, the values of σ_{ac}' and σ_{ac}'' decreased by adding Cr_2O_3 to the alkali borate compounds due to the blocking effect of the mobility of lithium and sodium ions by the presence of chromium ions,

III-2-3) Frequency Dependence of AC-Electrical Conductivity

Following Jonscher's power law, the real part of the ac electrical conductivity σ_{ac}' is given by equation (6) [26]:

$$\sigma_{ac}' = \sigma_{dc} + A\omega^s \qquad\qquad\qquad (6)$$

and

$$\sigma_{ac}' = A.\omega^s \qquad\qquad 0 \leq s \leq 1 \qquad\qquad (7)$$

Where σ_{dc} is the value of the dc-conductivity, i.e., $\sigma_{dc} = \sigma'(\omega \to 0)$, ω is the angular frequency ($\omega = 2\pi f$), A is the pre-exponential factor and s is the power-law exponent representing the degree of interaction between the mobile ions. In the high-frequency region, $A.\omega^s \geq \sigma_{dc}$, so the total conductivity is equal to the ac- conductivity [27]. In figure 8 and figure 9, the logarithmic relation between the measured values of σ_{ac}' and the applied frequency, ω, obtained at different temperatures are shown for all samples under consideration (see Table 3.1), respectively. From these figures, we notice that the conductivity increases by increasing the temperature. This effect is due to the increase of the ion mobility within the glass matrix. For all samples, conductivity shows a weak dependence on the frequency at lower values up to 10 kHz, after that shows a sharp increase with frequency. This effect may be attributed to the change in the type of polarization from space charge to ionic as the frequency increase. At every constant temperature, two distinct regions at low and high frequency are identified. In the low-frequency range, it is observed that the value of the electrical conductivity slightly changes and is called the dc-conductivity (σ_{dc}). The value of the σ_{dc} conductivity is referred to the long-range ion transport from their equilibrium positions 2. In the second region at higher frequencies, the curves features of Figure 8 and Figure 9 showed a linear relation between log σ_{ac}' versus log ω, where the conductivity increased with frequency at any temperature. The value of the exponent s was determined from these linear relations and found to be $0.9 < s < 0.99$. This frequency dependence arises from the forward-backwards jumps of ions, which are only measurable at small time scale (high frequency). Also, we noticed that at a higher frequency, the spectral curves of different temperatures tend to merge into a single curve.
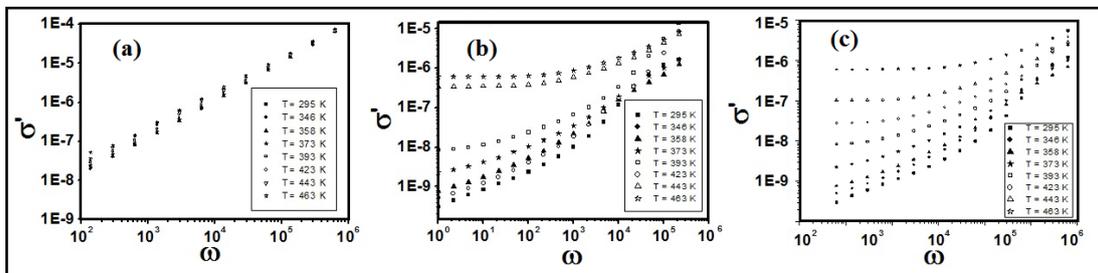

Figure 8: Variation of log σ_{ac} as a function of angular frequency (ω) at different temperatures for
    a)   **Pure lithium borate glass [37 mol %Li₂O +63 mol% B₂O₃] sample1**
    b)   **[37 mol % Li₂O +62.9 mol % B₂O₃+ 0.1 mol % Cr₂O₃] sample2**
    c)   **[37 mol % Li₂O +62.3 mol % B₂O₃+ 0.7 mol % Cr₂O₃] sample3**
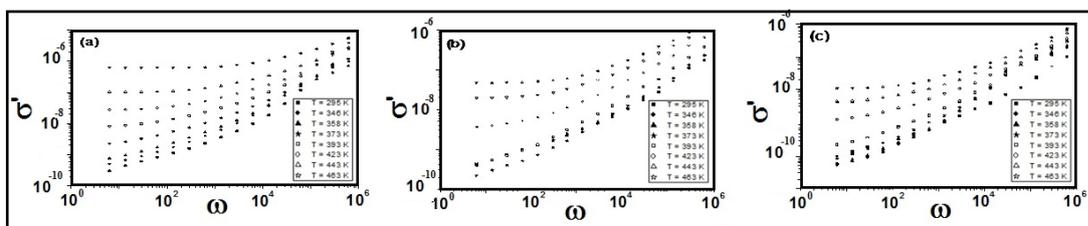

Figure 9: Variation of log σ_{ac} as a function of angular frequency (ω) at different temperatures for
    a)   **Pure sodium borate glass [22 mol% Na₂O +78 mol%B₂O₃] sample4**
    b)   **[37 mol % Na₂O +62.9 mol % B₂O₃+ 0.1 mol % Cr₂O₃] sample5**
    c)   **[37 mol % Li₂O +62.3 mol % B₂O₃+ 0.7 mol % Cr₂O₃] sample6**

III-3) Measurement of the Dielectric constant

We examined the dielectric response of all glass samples under consideration (see Table 1) by measuring both the real (ε') and imaginary (ε'') parts of the dielectric constant. In Table 2, the values of ε' and ε'' at room temperature and different frequencies are collected, respectively. At frequency 100 Hz the values of (ε') and (ε'') are equal to 15.23 and 6.07 for sample 1 and equal to 10.62 and 0.42 for sample 4, respectively. It is worth mentioning that these values are decreased by increasing the applied frequency. The variation of ε' and ε'' as a function of temperature at different frequencies of [37mol % M_2O +63mol % B_2O_3], [37mol % M_2O + 62.9mol% B_2O_3+0.1mol % Cr_2O_3] and [37mol % M_2O + 62.3mol% B_2O_3+0.7mol % Cr_2O_3] glass samples are illustrated in Figure 10 (with M= Li) and in Figure 11 (with M= Na), respectively.
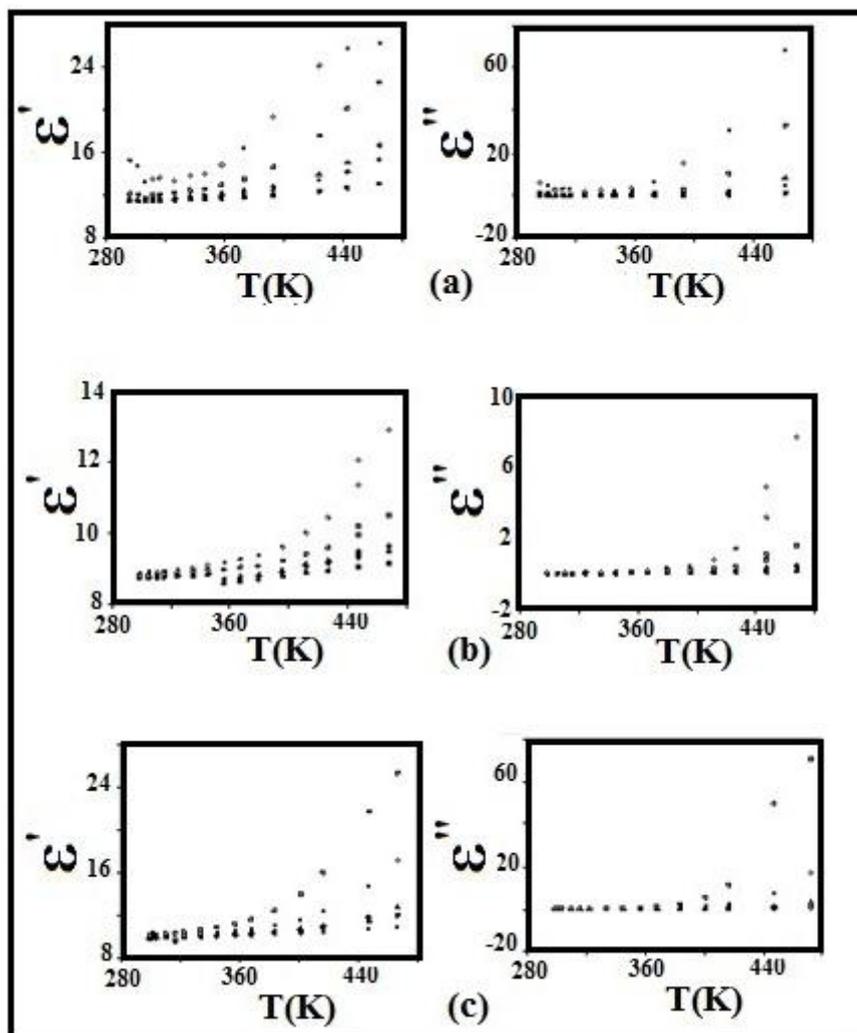

Figure 10: Variation of the real (ε') and imaginary (ε'') part of the dielectric constant as a function of temperature for:
a)   [37mol % Li_2O +63mol % B_2O_3] glass sample,
b)   [37mol % Li_2O + 62.9mol% B_2O_3.+0.1mol % Cr_2O_3] glass sample
c)   [37mol % Li_2O + 62.3mol% B_2O_3+ 0.7mol % Cr_2O_3]glass sample
○ 0.1KHz   □1 KHz   ▲10 KHz   ■ 100 KHz   ● 200 KHz
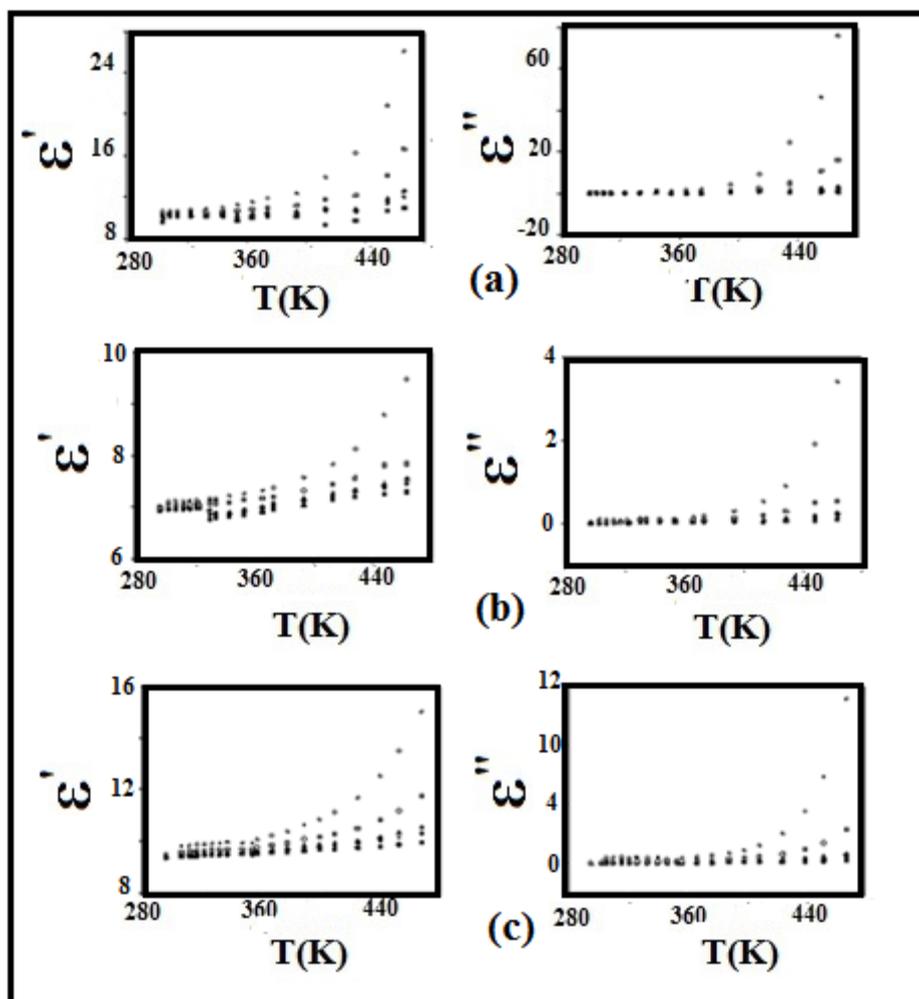
Figure 11: Variation of the real (ε') and imaginary (ε") part of the dielectric constant as a function of temperature for:

a) **[37 mol% Na_2O + 63mol % B_2O_3] glass sample**
b) **[37 mol % Na_2O + 62.9 mol % B_2O_3+ 0.1 Cr_2O_3] glass simple**
c) **[37 mol % Na_2O +62.3 mol % B_2O_3+0.7 Cr_2O_3] glass sample**
  ○ 0.1kHz   □1 kHz   ▲10 kHz   ■ 100 kHz   ● 200 kHz)

It is worth mentioning that at T > 400 K the values of ε' and ε" of the undoped alkali borate samples1 and sample4 are increased by increasing the temperature. This effect is referred to as the charge accumulation at the surface of the electrodes [1]. We may attribute the increase of ε' and ε" values of the doped samples to the decrease in the magnitude of space charge polarization. Possibly it may be referred to the presence of a part of chromium ions in Cr^{6+} state that participates in the network forming with CrO_4 structural units. At this particular low concentration Chromium ions mostly exist in Cr^{3+} state, which acts as modifiers. This modifier creates bonding defects by breaking B-O-B, B-O-Cr, etc., which may create accessible pathways for the migration of charges that would build up space charge polarization and lead to an increase in the dielectric parameters as observed. Figure 12 and Figure 13 show, respectively, the variation of ε' and ε" as a function of the applied frequency for lithium and sodium borate glasses (see Table 1) at different temperature.

It is observed that the value of ε' and ε" decreased by increasing the frequency at any temperature. In the undoped lithium and sodium borate glasses (samples1 and sample 4), the dielectric losses are mainly attributed to the Li and Na ion conduction, respectively. For comparison, the results of ε' and ε" at T = 293 K for all doped glass samples number 2, 3, 5, and 6 glasses containing a low concentration of chromium oxide are collected in Table 2. It is worth to mention that the value of the dielectric loss is attributed to the ion jump, conduction loss of ions and ion polarization loss [27]. We noticed that the dielectric constant and dielectric losses of these samples decreased by 30-60% less than the corresponding values obtained for the undoped lithium and sodium borate glasses (samples1 and sample 4), respectively. This behaviour is attributed to the presence of the chromium ions in the divalent state within the glass matrix [28-30].
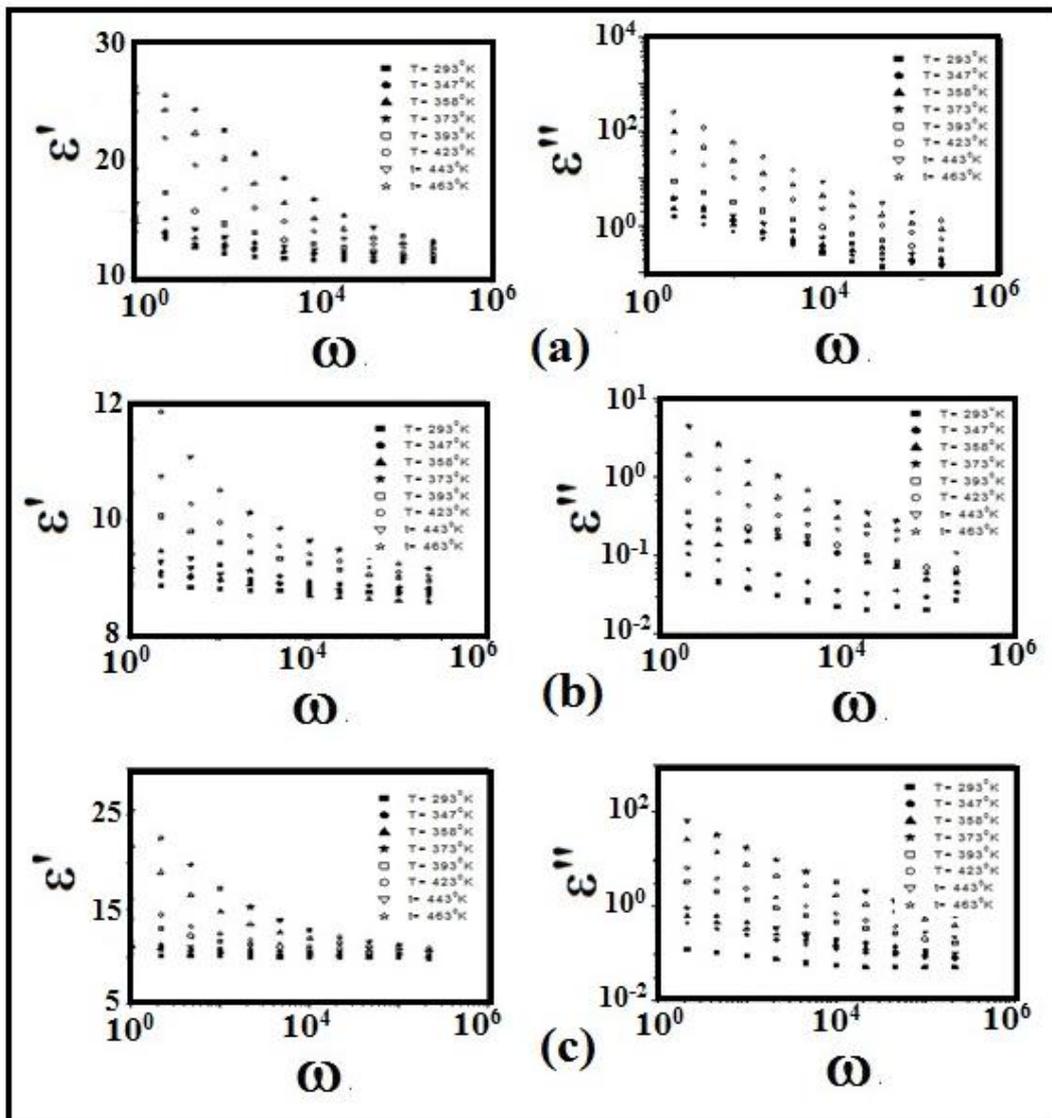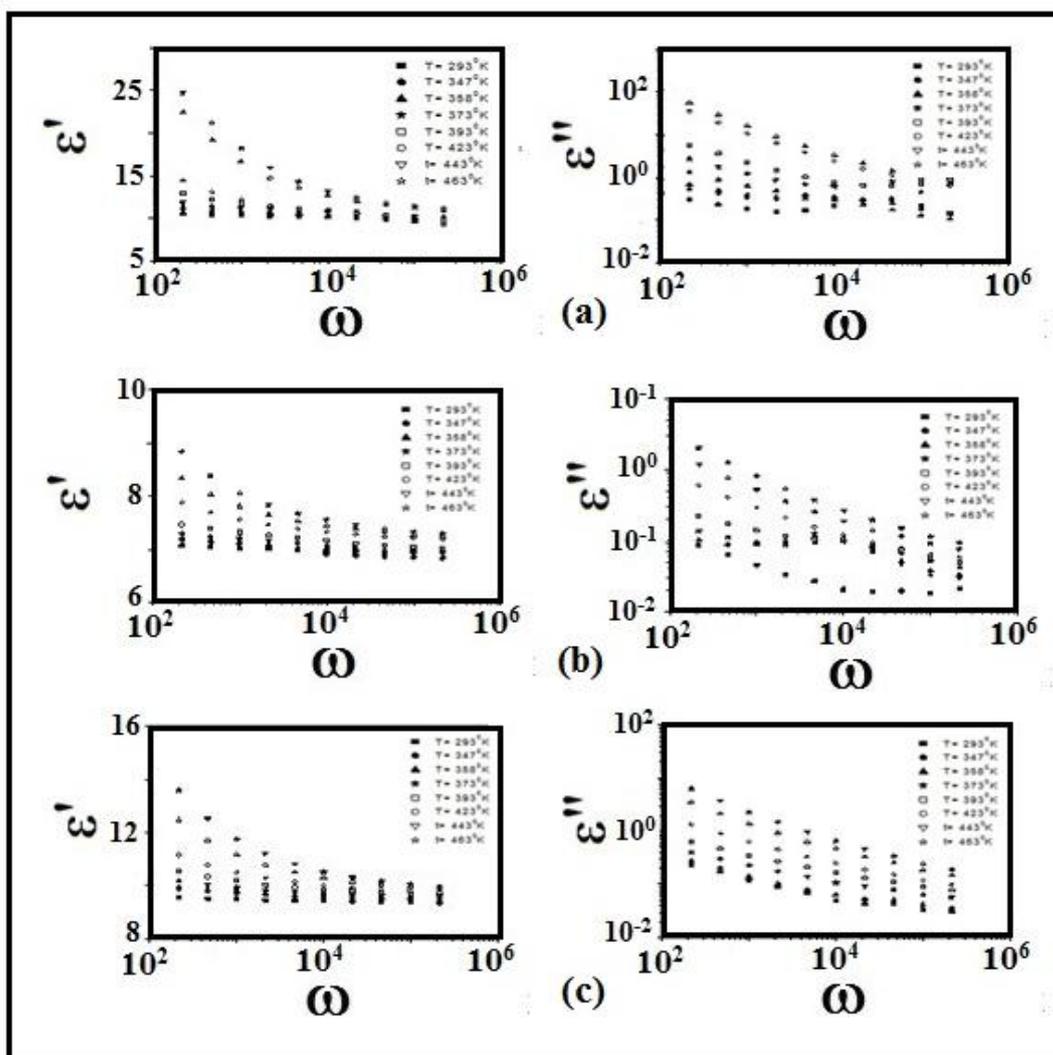
Figure 12: Variation of the real (ε') and imaginary (ε'') part of the dielectric constant as a function of frequency at different temperatures for:
  a) [37mol % Li_2O +63mol % B_2O_3] glass sample,
  b) [37mol % Li_2O + 62.9mol% B_2O_3.+0.1mol % Cr_2O_3] glass sample
  c) [37mol % Li_2O + 62.3mol% B_2O_3+ 0.7mol % Cr_2O_3]glass sample

Figure 13: Variation of the real (ε') and imaginary (ε") part of the dielectric constant as a function of frequency at different temperatures for:
   a) **[37 mol% Na$_2$O + 63mol % B$_2$O$_3$] glass sample**
   b) **[37 mol % Na$_2$O + 62.9 mol % B$_2$O$_3$+ 0.1 Cr$_2$O$_3$] glass simple**
   c) **[37 mol % Na$_2$O +62.3 mol % B$_2$O$_3$+0.7 Cr$_2$O$_3$] glass sample**

IV. Conclusions

In this report, we introduced a low concentration of Cr$_2$O$_3$ has been to some alkali borate glasses. The glass samples were successfully prepared by the melt quenching method.

In conclusion, the results showed the following:
   a) From the recorded XRD Spectra, the nature of the amorphous nature of these glass samples was observed. Evidence of the formation of pre-crystalline phase was found.
   b) The values of the ac-conductivity of the undoped samples are affected by the existence of different physical and chemical processing.
   c) At low temperature (T < 400 K) the ion-ion interaction and the formation of different complexes may play an essential role in decreasing the value of the electrical conductivity.
   d) At high temperature (in the crystalline stage T > 400 K) the main contribution to the conductivity is attributed to the electron hopping mechanism.
   e) The conduction mechanism for doped samples is affected by the blocking effect of the mobility of Li and Na ions by the presence of chromium ions.
   f) At T < 400 K, deviation from the Arrhenius linear model was found. Neither the polaron hopping nor the variable range hopping models explain this behaviour.
   g) The scaling law of the ac-conductivity as a function of frequency was verified.

h) The large capacitance at the electrode surface and the increase of the ionic mobility are responsible for the behaviour of the dielectric loss of these glass samples.

Acknowledgement

References

[1]. J. Habaski, C. León, K.L. Ngai, Dynamics of glassy, crystalline and liquid ionic conductors, Springer International Publishing, Switzerland, (2017), Ch.4. http//DOI: 10.1007/978-3-319-42391-3

[2]. K. Funke, Progress in physical chemistry: Ionic motion in materials with disordered structures from elementary steps to macroscopic transport, Oldenbourg Wissenschftsverlag, GmbH, München, Germany, 4, (2011), 223-244.

[3]. L. Wu, A. Koryttseva C.B.M Groß, A. Navrotsky, Thermochemical investigation of lithium borate glasses and crystals, J. Am. Ceram. Soc., (2019), 102[8], 4538-4545. https://doi.org/10.111/jace.16323

[4]. S.S. Sørensen, H. Johra, J.C. Mauro, M. Bauchy, M. Morten, M.M. Smedskjaer. Boron anomaly in the thermal conductivity of lithium borate glasses, Physical Review Materials, (2019), 3[7], 075601. DOI: 10.1103/PhysRevMaterials.3.075601

[5]. V. Montouillout, H. Fan, L. Campo, S. Ory, A. Rakhmatullin, F. Fayon, M. Malki, Ionic conductivity of lithium borate glasses and local structure probed by high-resolution solid-state NMR, Journal of Non-Crystalline Solids, 484, (2018), 57-64. DOI: 10.1016/j.jnoncrysol.2018.01.020

[6]. V.L. Usharani, B. Eraiah. Thermal property of holmium doped lithium lead borate glasses, AIP Conference Proceedings, (2018), 1951, 020004. DOI: 10.1063/1.5031712

[7]. P. P. Pawar, S. R. Munishwar, S. Gautam, R.S. Gedam, Physical, thermal, structural and optical properties of Dy^{3+} doped lithium alumino-borate glasses for bright W-LED, Journal of Luminescence, (2017), 183, 79-88. https://doi.org/10.1016/j.jlumin.2016.11.027

[8]. V. Thakur, A. Singh, A. M. Awasthi, L. Singh. Temperature-dependent electrical transport characteristics of BaTiO3 modified lithium borate glasses, AIP Advances, (2015), 5, 087110. https://doi.org/10.1063/1.4928339

[9]. Kh. Shaaban, S.M. Abo-Naf, M. E. M. Hossouna, Physical and Structural Properties of Lithium Borate Glasses Containing MoO_3, Springer Science + Business Media, Dordrecht, Silicon, (2017). DOI 10.1007/s12633-016-9519-4

[10]. A. Abousehly, S.A.M. Issa, M.A. El-Oyoun, N. Afify, Electrical and mechanical properties of Li2O–BaO–B2O3 glass system, J. Non-Cryst. Solids, (2015), 429, 148–152. http://dx.doi.org/10.1016/j.jnoncrysol.2015.09.003.

[11]. T. Maheswari, V. Naresh, R. Ramaraghavulu, S. Buddhudu, B. H. Rudramadevi, Studies on Thermal and Spectral Properties of Ho^{3+}: Lithium Borate Glasses, International Journal Of Engineering Research & Technology (IJERT), (2014), 3[7], 574-580.

[12]. J. Anjaiah, C. Laxmikanth, P. Kistaiah, N. Veeraiah, Dosimetric and kinetic parameters of lithium cadmium borate glasses doped with rare-earth ions, Journal of Radiation Research and Applied Sciences, (2014), 7[4], 519-525. https://doi.org/10.1016/j.jrras.2014.08.009

[13]. V. Naresh, S. Buddhudu, Structural, thermal, dielectric and ac conductivity properties of lithium fluoro-borate optical glasses, Ceramics International, (2012), 38[3], 2325-2332.https://doi.org/10.1016/j.ceramint.2011.10.084

[14]. R. S. Gedam, D. D., Ramteke, Electrical and optical properties of lithium borate glasses doped with Nd2O3, journal of rare earths, (2012), 30[8], 785–789. DOI: 10.1016/S1002-0721(12)60130-6

[15]. K. Funke, R.D. Banhatti, Modelling frequency-dependent conductivities and permittivities in the framework of the MIGRATION concept, Solid State Ionic, (2004), 169[1-4], 1-8. https://doi.org/10.1016/j.ssi.2003.06.003

[16]. M. A. Zaki Ewiss, Electrical, infrared spectroscopy and DTA studies of some sodium tetraborate glasses containing Fe_2O, Phys. Chem. Glasses, (1998), 39[4], 236-240.

[17]. M. A. Zaki Ewiss, S. A. Abu Mansoor, Electrical, I.R. spectroscopy, and DTA studies of some sodium tetraborate glasses containing vanadium oxide, Physica status solidi (a), (1996), 156[2], 421-431. https://doi.org/10.1002/pssa.2211560220

[18]. M. A. Zaki Ewiss, M. Y. El Zayat, R. Nothhelfer-Richter, Dielectric spectroscopy of $[(Na_2B_4O_7)98\%-(Cr_2O_3)2\%]$ and $[(Na_2B_4O_7)98\%-(MnO)2\%]$ semiconductor glasses, Physics and Chemistry of Glasses, (2002), 43[3], 165-170.

[19]. H. M. Kamari et al., Optical Properties of Lithium Borate Glass (Li2O)x (B2O3)1-x, Sains Malaysiana, (2014), 43[6], 899-902.

[20]. I.G. Austin, N.F. Mott, Polarons in crystalline and non-crystalline materials. Adv Phys, (1969), 18, 41–102.

[21]. G.N. Greaves, S.J. Gurman, C.R.A, Catlow, A.V. Chadwick, S. Houde-Walter, C.M.B. Henderson, D.B. Dobson, A structural basis for ionic diffusion in oxide glasses, Philos. Mag. A, (1991), 69. https://doi.org/10.1080/01418619108204878

[22]. S.W. Martin, D.M. Martin, J.A. Schrooten, B.M. Meyer, Trapping model for the non-Arrhenius ionic conductivity in fast ion-conducting glasses, Journal of Physics: Condensed Matter, (2003), 15[16]. https://doi.org/10.1088/0953-8984/15/16/312

[23]. Q. Mei, Structural investigation into the non-Arrhenius behaviour of fast ion conducting sulfide glasses, Retrospective Theses and Dissertations, (2003). 606, Iowa State University. https://lib.dr.iastate.edu/rtd/606

[24]. Y.H. Elbashar, A.M. Badr, H.A. Elshaikh, A.G. Mostafa, A.M. Ibrahim, Dielectric and optical properties of CuO containing sodium zinc phosphate glasses, Processing and Application of Ceramics, (2016), 10[4], 277–286. DOI: 10.2298/PAC1604277E

[25]. M.P.F. Graça, B.M.G. Melo, P.R. Prezas, M.A. Valente, F.N.A. Freier, L. Bih, "Electrical and dielectric analysis of phosphate-based glasses doped with alkali oxides", Mater. Design, (2015), 86, 427–435. https://doi.org/10.1016/j.matdes.2015.07.043

[26]. V. P. Seth, A. Yadav, S. K. Gupta, Electrical conductivity and ESR of lithium borate glasses containing mixed transition metal oxides. J Mater Sci, (1988), 23, 3495–3500. https://doi.org/10.1007/BF00540485

[27]. A.K. Jonscher, The universal dielectric response. Nature, (1977), 267, 673-679. https://doi.org/10.1038/267673a0

[28]. I. Stavrakas, K. Moutzouris, K. Ninos, N. Mitritsakis, Z. Agioutanatis, D. Triantis, Using A.C. conductivity measurements to study the influence of mechanical stress on the strength of geomaterials, Open J. Appl. Sci., (2012), 2, 61–65. DOI: 10.4236/ojapps.2012.22007

[29]. A. E. Bekheet. Ac-conductivity and dielectric properties of Ga_2S_3-Ga_2S_3 film. Physica B, (2008), 403, 4342-4346.

[30]. S. Thomas, R. George, M. Rathaiah, V. Venkatramu, Sk. N. Rasool, N. V. Unnikirshnan. Structural vibrational and dielectric studies of Sm^{3+}-doped K-Mg-Alzincfluorophosphate glasses. Physica B, (2013), 431, 69-74.